JOURNAL OF MATERIALS SCIENCE **36** (2001) 1717–1725

Diffusion controlled precipitation of austenitic bi-crystals possessing twin related orientation in the ferrite of a duplex stainless steel

A. REDJAÏMIA, G. METAUER
Laboratoire de Science et Génie des Surfaces, UMR-CNRS 7570, Ecole Européenne d'Ingénieurs en Génie des Matériaux, Ecole des Mines, Parc de Saurupt, 54042 Nancy Cedex, France
E-mail: redjamia@mines.u-nancy.fr

The ferritic matrix in the Fe-22Cr-5Ni-3Mo-0.03C ferritic-austenitic duplex stainless steel can undergo a variety of decomposition processes when aged in the temperature range 650–550°C. One of these processes is the formation of austenite in the shape of a spearhead. Unlike the one found at high temperature, this austenite is characterized by a habit plane, which is similar to the midrib of the martensite. This feature suggests that a diffusionless process as referred to in the literature controls its formation. In the present investigation, transmission electron microscopy (TEM) and energy dispersive X-ray spectroscopy (EDS) results indicate that the proposed precipitation mechanism must be reviewed. Based on the crystallographic results in conjunction with the clear-cut difference in chemical composition between the matrix and the austenitic second phase, the equilibrium shape is explained and the ambiguity of precipitation mechanism has been brought to light. It has been suggested that the latter one goes through the following steps: (i) enrichment of the (110)-ferritic planes with γ-forming elements by diffusion, (ii) double shear to transform (110)-ferritic planes into (111)-austenitic planes, i.e., to change from BCC (δ) to FCC (γ), (iii) twinning of the FCC γ structure to reduce local strains and formation of γ bi-crystals and (iv) growth of the twinned γ towards the ferritic matrix by volume diffusion.

1. Introduction

Duplex stainless steels are being increasingly used as structural material in oil, chemical and power industries [1–4]. This is related to the fact that their duplex microstructure ($\delta + \gamma$) allows a beneficial combination of austenitic (γ) and ferritic (δ) properties: on the one hand high strength with a desirable toughness [5, 6] and, on the other hand, good corrosion resistance, especially to chloride-induced stress corrosion cracking [7–9]. The Z3CND-22-05, of nominal composition (wt%) Fe-22Cr-5Ni-3Mo-0.03C is a member of this family. It has an excellent potential for application in offshore conditions [10]. The heat treatment of this duplex stainless steel leads to a series of metallurgical transformations which take place in the ferrite or at its grain boundaries, apart from the martensite which forms in the austenite [11, 12]. In a detailed study [13], efforts were made to characterize the different products of the δ ferrite matrix decomposition in the temperature range 1050–400°C. The characterization of the phase precipitation was best undertaken by isothermal heat treatment from the fully δ ferrite microstructure retained by water quenching at ambient temperature from the solutionizing single domain. This isothermal treatment induces the decomposition of the supersaturated δ ferrite. The various identified phases include $M_{23}C_6$ type carbides, austenite (γ), the α' BCC ferrite [14] being responsible for the well-known embrittlement at 475°C in Fe-Cr system [15], the intermetallic G-phase [16], the novel τ-phase described elsewhere [17] and the undesirable topologically close-packed (TCP) phases. The latter being mainly the Frank-Kasper phases: sigma (σ), khi (χ) and R [18].

As part of the continuing investigation, an isothermal heat treatment, in the temperature range 650–550°C for various durations up to 336 hours, leads to very fine precipitates throughout the δ matrix. These precipitates, completely identified by convergent beam electron_diffraction (CBED) as austenite, belong to the $Fm3m$ space group [13]. This austenite, morphologically different from the one found at high temperature, takes place in addition to the intermetallic compounds R and τ. Due to its spearhead-like morphology, this austenite is labelled γ_s. The γ_s particles are characterized by a habit plane, which is similar to the midrib of the martensitic austenite referred to in a previous study [19], which suggested that the precipitation is controlled by a diffusionless transformation. In duplex steel with a close chemical composition, Southwick and Honeycombe [20] have identified a very

fine precipitation with heavily faulted particles, whose transformation mechanism is also a martensitic one. However, our crystallographic results and the significant difference in chemical composition between the δ matrix and γ_s indicate that the proposed precipitation mechanism of this second phase must be reviewed. It is intended through this study to characterize this austenite to explain its equilibrium shape and to overcome the ambiguity of the formation mechanism, by using transmission electron microscopy (TEM) coupled with energy-dispersive X-ray spectroscopy (EDS).

2. Material and experimental procedure

The as-received Fe-22Cr-5Ni-3Mo-0.03C (wt%) duplex austenitic-ferritic ($\delta + \gamma$) specimens were solution treated at 1375°C for 20 min to achieve homogeneity and subsequently water quenched to retain a supersaturated and fully ferritic (δ) microstructure. Specimens were then treated in the temperature range 650–550°C for various durations up to 336 hours, followed by water-cooling. All the heat treatments were carried out in electric muffle furnaces under vacuum to minimize oxidation.

Thin foils were prepared for transmission electron microscopy (TEM) by grinding the metallographic samples to 20 μm thickness and by double jet electropolishing in a solution of 5% perchloric acid in 95% II-butoxyethanol at 40 V potential. They were investigated in two transmission electron microscopes. The Philips CM 12 operated at 120 kV and the Jeol 200 CX operated at 200 kV. They employed double-tilt goniometer stages, which could be tilted ($\pm 60°$) for two orthogonal directions. The diffraction patterns were obtained in convergent beam electron diffraction (CBED) mode with a nearly parallel electron beam focussed on a very small area of the thin foil. High-resolution electron microscopy (HREM) was performed on a Philips EM 430 ST electron microscope operated at 300 kV. The optimum point-to-point resolution was better than 0.2 nm. This instrument was equipped with a Tracor-Northern energy-dispersive X-ray spectroscopy (EDS) analysis system. The EDS spectrometer is interfaced with a minicomputer to log the spectra and to conduct qualitative or quantitative analyses. Quantitative analysis of EDS spectra without standards was performed assuming the thin film approximation of no absorption. The Cliff-Lorimer expression for concentration ratios was used, relying on k values calculated for K spectral lines.

3. Experimental results

3.1. Structure of γ_s–phase

The result of the isothermal heat treatment, in the temperature range 650–550°C, originates in very fine precipitates (less than 0.5 μm) throughout the δ matrix (Fig. 1). These precipitates, identified by Convergent Beam Electron Diffraction (CBED), belong to the $Fm\bar{3}m$ space group [13]. Characterised by X-ray diffraction, the δ matrix parameter, $a_\delta = 0.2867$ nm, is used as a calibration to find that the lattice constant of the austenite is $a_\gamma = 0.359$ nm [13]. Particles adopt a spearhead-like morphology (Fig. 1) with a habit plane similar to the midrib of the martensite. This habit plane and the growth direction of the γ_s particles were determined by trace analysis. Such analyses, involving several orientations of δ matrix grains, established that the median plane and the growth direction of the particles are $\{110\}\delta$ and $\langle 112\rangle\delta$, respectively. Thus the deduced

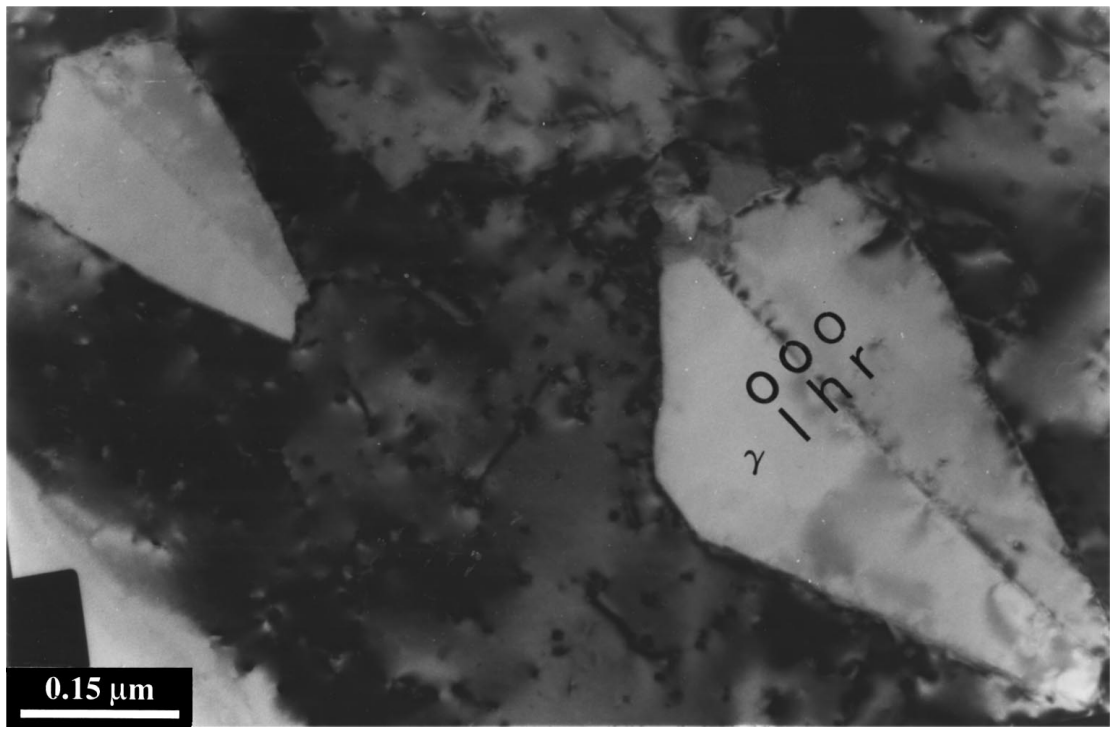

Figure 1 Bright field TEM micrograph showing twin-related γ_s particles embedded in the surrounding δ matrix. The median line, exhibited by every γ_s particle, is the trace of the twinning plane.

number of the particle variants developed in a given grain, is equal to twelve ($n = 12$).

3.2. Orientation relationship and morphology analysis: The equilibrium shape

The γ_s-phase crystal lattice is oriented with respect to the surrounding δ matrix according to the well-known Kurdjumov-Sachs (K-S) orientation relationship as deduced from the recorded electron diffraction patterns (Fig. 2). This orientation relationship, which consists in making the close-packed planes parallel, may be specified by one of the 24 possible variants as:

$$(111)\gamma_s//(011)\delta$$
$$[-101]\gamma_s//[-1-11]\delta$$
$$[-12-1]\gamma_s//[-21-1]\delta$$

It is well established that the morphology of transformation products, taking place in a solid matrix by diffusion-controlled mechanism or diffusionless mechanism (martensitic transformation), is of great importance in materials science. Understanding of both the equilibrium shape and the habit plane adopted and developed between the transformation products and the parent phase has been widely investigated. In the martensitic transformation, the optimum shape prediction has successful. For diffusion-controlled mechanism, several models [21–23] have been proposed and the morphology prediction, in the centre of the present study, has been of limited success.

Both the morphology and the variant number of the precipitate, which adopts orientation relationships with the matrix, can be understood in terms of the group theory [24, 25]. This approach, based on the shared symmetry elements of the two point groups of product and parent phases, is applied here to explain γ_s–phase precipitation features.

First of all, let us consider G^δ and G^{γ_s} to be the symmetry point groups of the ferritic matrix and the decomposition product, the γ_s–phase, respectively. The intersection point group of $G^\delta = m\bar{3}m$ and $G^{\gamma_s} = m\bar{3}m$ is represented by their common symmetry elements when the precipitate adopts an orientation relationship with the matrix [24, 25]. This intersection point group, labelled H ($H = G^\delta \cap G^{\gamma_s}$), is one of the 32 crystallographic point groups and a subgroup of the matrix and of the precipitate point groups. Cahn and Kalonji [25] assert that it is an error to relate the morphology of the precipitate to the symmetry of the matrix or of the precipitate. They suggest that the precipitate crystal adopts a form consistent with the symmetry of the subgroup H. Another important concept of the crystallographic symmetry is the index of the subgrouping which provides the number of precipitate variants of a given orientation relationship. Defined as the index of H in G^δ, the number of variants is the ratio of the order of G^δ to the order of H. The order of each point group represents its symmetry element number [26]. This symmetry concept has been successfully applied to determine the number of variants and to characterize the morphology of precipitates in different alloy systems [27, 28].

According to the K-S orientation relationship developed by the γ_s–phase with the δ matrix, both belonging

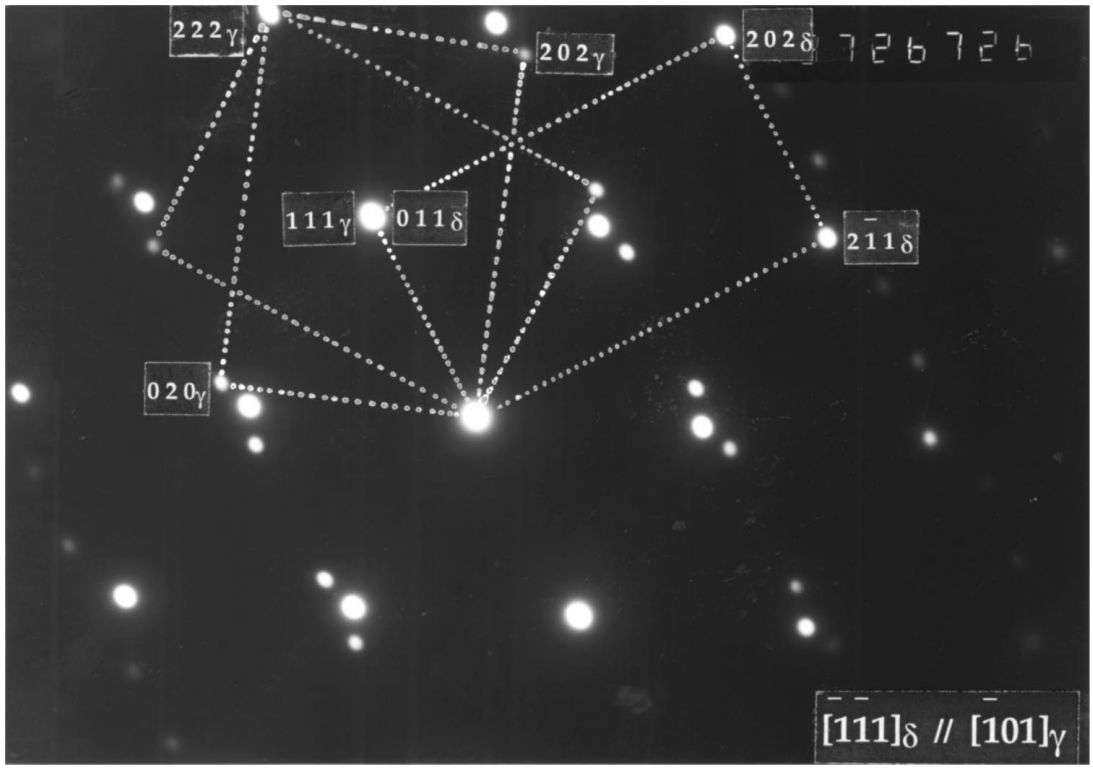

Figure 2 Composite diffraction pattern recorded along $[-1-11]\delta//[-101]\gamma$ zone axis compound of three patterns: one of them corresponds to $[-1-11]\delta$ and the others to two twin related patterns along $[-101]\gamma$. Notice the K-S orientation relationship between the two variants of γ_s and the δ matrix.

TABLE I Determination of the intersection point group H, the symmetry elements of which are common to the γ_s austenite and the δ matrix

K-S Orientation relationship	Superimposed symmetries	Shared symmetries
$(111)\gamma_s//(011)\delta$	3 on $2/m$	
$[-101]\gamma_s//[-1-11]\delta$	$2/m$ on 3	1
$[-12-1]\gamma_s//[-21-1]\delta$	1 on 1	

to the same point group $m\bar{3}m$, the results of the symmetry analysis are summarized in Table I.

For the K-S orientation relationship, 3 and $2/m$ rotation axes are lost and the only surviving symmetries are superimposed inversion centres. It is therefore clear that the shared symmetry elements lead to the intersection point group H:

$$H = G^{\delta} \cap G^{\gamma_s} = \frac{4}{m}\bar{3}\frac{2}{m} \cap \frac{4}{m}\bar{3}\frac{2}{m} = \bar{1}$$

The resulting intersection point group $H = \bar{1}$, the triclinic point group the order of which is 2, dictates the shape of γ_s particles. For this point group, there is no special form and the equilibrium shape is a pinacoid [29]. This predicted form is consistent with the one experimentally observed.

Defined as the index of H in G^{δ}, the number of variants is the ratio of the order of G^{δ} to that of H, i.e., $48/2 = 24$ [24, 25]. This means that for the γ_s-phase, there are 24 variants that could take place in every grain of the matrix. This variant number deduced from the K-S orientation relationship analysis is not in agreement with the one determined by trace analysis. To overcome this ambiguity, the diffraction pattern (Fig. 3), recorded only from γ_s particle, is considered. This diffraction pattern, obtained along $[-101]\gamma_s$, is compound of two patterns. The analysis of the reflections indicates that the latter are twinned austenite diffraction patterns. These results, sustained by different bright field and dark field experiments, clearly indicate that γ_s particles are compound of two twin-related variants, i.e., two particles with the same habit plane: the twinning plane $(111)\gamma_s//(011)\delta$. The two variants develop symmetrically from the twinning plane. Thus, the variant number 12, obtained in Section 3.1, by trace analysis, eventually becomes (12×2) 24, and agrees with the one deduced from the K-S orientation relationship in conjunction with the group theory. This result is corroborated by the fact that γ_s particles were also found with only one variant (Fig. 4), whose shape is a pinacoid belonging to $\bar{1}$ point group [29]. However, this morphology is rarely observed. It is interesting to notice that the particles with one untwinned variant are much more developed than the ones compound with twin-related particles.

The shape of γ_s–phase is dictated by the triclinic intersection point group $H = \bar{1}$ which is characterized by no symmetry-dictated extremum [24, 25]. This is not surprising because the exact K-S relationship is never observed. Indeed, a deviation from K-S has been observed in different systems. Its occurrence corresponds to symmetry-dictated extrema

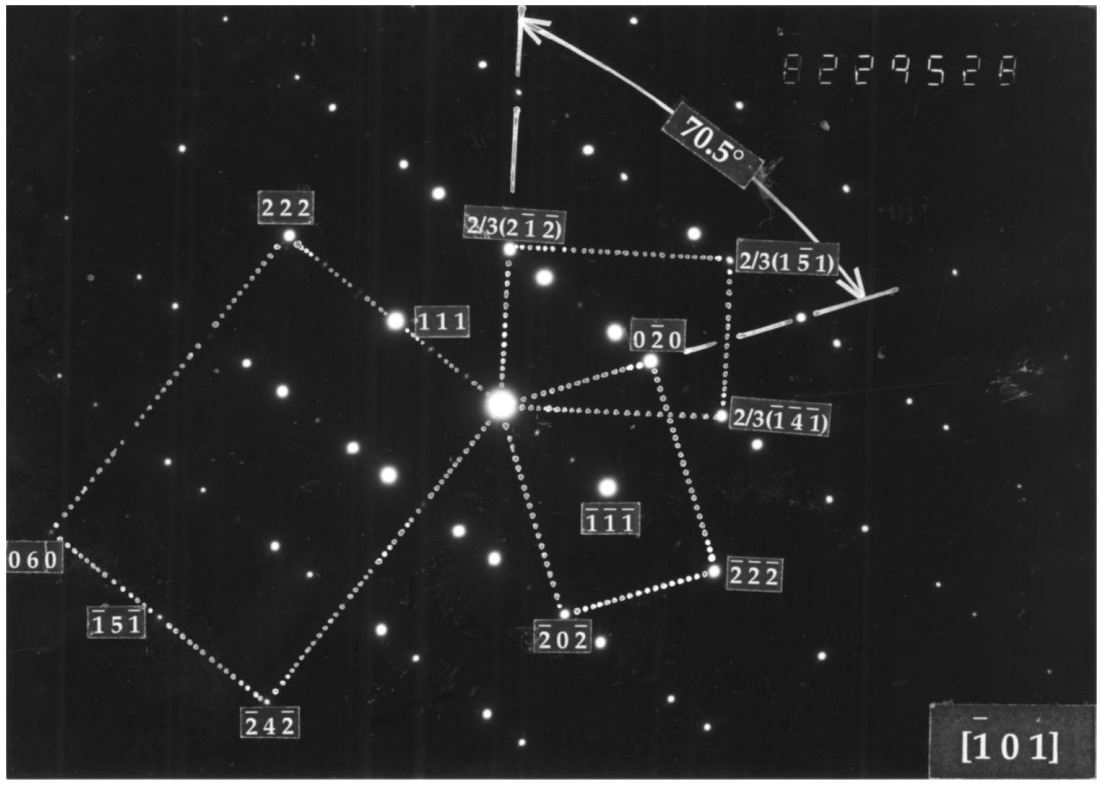

Figure 3 The composite diffraction pattern, recorded along $[-101]\gamma_s$ corresponds to the patterns of two twin-related variants of γ_s particle. The dashed unit cells, in the reciprocal lattice, defined with {[−20−2], [0−20], [−202]} and {2/3[−1−4−1], 2/3[2−1−2], [−202]} vectors, correspond to the two twin-related variants. The dashed unit cells, defined with {[222], [−24− 2], [−202]} and {1/3[111], 1/3[−24−2], [−202]} vectors correspond, respectively, to the cells of the coincidence-site lattice (CSL) and the displacement shift complet (DSC) lattice of the reciprocal lattices of the two twin-related variants. Spots the intensity of which is weak are due to double diffraction.

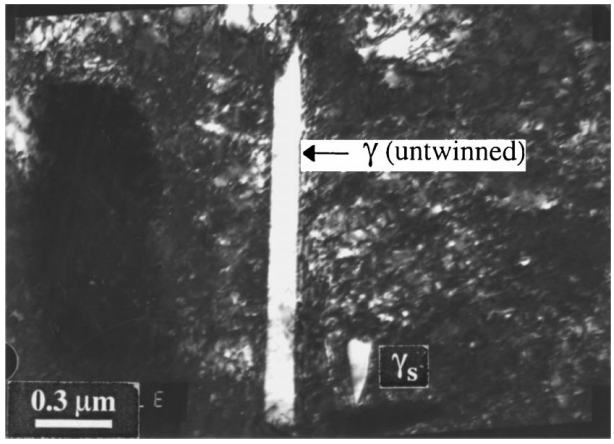

Figure 4 Bright field TEM micrograph showing two particles of austenite: one of them is untwinned and the other one exhibits twin-related variants. One can notice that the untwinned particle is much more developed than the one compound with the twin-related variants.

such as Nishiyama-Wasserman (N-W) and Bain orientation relationships. The latter lead to $H = 2/m$ and $H = 4/m\,2/m\,2/m$ respectively, both corresponding to symmetry-dictated extrema [24, 25]. In duplex stainless steels whose compositions are close to the one considered in this study, Southwick [30] and El Hajjaji [31] have reported 2.8° and 4° deviations to K-S relationship. However, Penisson *et al*. [32] have pointed out that the orientation relationships between the δ matrix and the austenite precipitating at high temperature are not constant and are varying in the domain contained between K-S and N-W relationships.

The symmetry-dictated extremum and the deviation to the exact K-S relationship will be dealt with in the next section.

3.3. The γ_s/δ interface

In the metallurgic systems, the FCC/BCC interface is one of the most important heterophase interfaces and the most widely investigated in detail [21, 22]. Their interest is intimately linked to the crucial role played in the control of the physical and mechanical properties of alloys. The equilibrium of these interfaces is assumed to be linked to the presence of intrinsic defects such as dislocations and ledges [33]. In order to prove evidence of the θ deviation from the K-S relationship, high-resolution electron microscopy observations have been undertaken in this study. HREM images have been recorded along $[-1-11]\delta//[-110]\gamma_s$, showing the heterophase interface between γ_s-phase and δ matrix. Unfortunately, these images are of insufficient quality to be presented in this paper. However, when the image is observed at a glancing angle, one can note, at the level of the interface, a weak misorientation between $(111)\gamma_s$ and $(011)\delta$, the measure of which is assessed to be smaller than 1°. The compact planes of the two phases are not exactly parallel. The swerving, at the interface, is assumed to be due to intrinsic dislocations. In different TEM images orientations, a regular array of dislocations is pointed out at the γ_s/δ interface. The $\Delta\theta$ misorientation reported elsewhere [31, 32] and the one found in this study, are related to the variation of the a_{FCC}/a_{BCC} parameters ratio and are localised, as established by Dahmen [23], between the exact N-W and K-S orientations. Referring to the lattice parameters of the two phases δ and γ, the parameters ratio is in agreement with the results indicated by Dahmen [23].

It has been established that the orientation, between the ferrite and the austenite in duplex stainless steels, is related to the alloy purity [31]. In high purity alloys, N-W orientation is the most frequently observed one. However, the addition of carbon and/or sulphur [31] modifies the interface structure by locally accommodating the structure and thus favouring the K-S orientation relationship to the detriment of the more stable N-W OR, which corresponds to a partial extremum dictated by the symmetry. Moreover, Luo *et al*. [34] pointed out that the phosphorus impurities and ageing heat treatment also have a marked influence on the morphology and on the crystallography of Cr precipitates in dilute Cu-Cr alloys.

3.4. Twin-related variants of γ_s-austenite in δ matrix

Let us treat briefly the twinning in the FCC structure and focus on the electron diffraction of the γ_s-austenite in the δ matrix.

Twinning, a phenomenon usually observed in ferrous alloys and steels, is of great importance in controlling mechanical properties. It occurs as a consequence of plastic deformation, recrystallisation or growth stress accommodation. From a geometrical point of view, a twin is a composite crystal (bi-crystals) the individuals of which are of the same species and are joined together in some definite symmetry operation.

In real space, the twin-related individuals (variants) of FCC structure are simply mirrored across (111) plane, i.e., the twin boundary. An alternative description of twinning is a 180° rotation about [111] direction, the twin plane normal. Consequently, the reciprocal lattices of the twin-related variants are related by a 180° rotation about the [111] direction. Numerous methods are available for directly indexing the twin-related spot diffraction patterns [36]. The diffracting planes indices of the twinned crystals can be readily related by the following transformation matrix [37]:

$$T_{111} = \begin{pmatrix} -1 & 2 & 2 \\ 2 & -1 & 2 \\ 2 & 2 & -1 \end{pmatrix}$$

T_{111} is the transformation matrix when the twinning occurs on (111) plane of the FCC structure.

The composite electron diffraction pattern (Fig. 3), obtained along $[-101]$, is compound of two diffraction lattices corresponding to the twin-related variants of austenite. A 180° rotation along [111], of the $[-101]$ spots pattern of one variant, will position the spots of the other one. The dashed unit cells defined with the two following triplets of reciprocal vectors: $\{[-20-2], [0-20], [-202]\}$ and $\{[2/3[-1-4-1], [2/3[2-1-2], [-202]\}$ correspond to two twin-related variants. The row of spots through the origin and

perpendicular to the twin plane (i.e. parallel to [111] reciprocal direction) and every third row are common to both twin-related variants. The fact that the third row is common to the two twin-related lattices, indicates that the studied twin is $\Sigma 3$ grain boundary characterised by a 70.53 rotation around [−101] zone axis, as indicated in Fig. 3. The index $\Sigma = 3$ is the multiplicity of the coincidence-site lattice (CSL) [38] in the real space and is the ratio between the volume of the CSL unit cell and the volume of the crystal unit cell.

In interpenetrating twins, the twin variants develop an interface, the twin boundary, and lead to the coincidence-site lattice and related lattices [38]. It is well known that most materials of technological interest are used in their polycrystalline state. Their mechanical and chemical properties are controlled to a great extent by the interface between crystallites. Since the energy of polycrystal is higher than that of monocrystal with the same mass, the excess energy is stored in the interface and is related to the orientation of the neighbouring grains. The best properties of these materials are connected to the optimisation of the grain size and the quality of the interfaces. The latter is based on the properties of coincidence-site lattice (CSL) and related lattices, i.e., the displacement shift complete (DSC) lattice [38]. Based on the geometry of the latter lattices, it is possible to have access to the possible dislocations Burger vectors of the interface.

For this purpose, the composite diffraction pattern recorded along [−101] (Fig. 3) shows the CSL and DSC reciprocal lattices of the two twin-related variants. The dashed unit cells of these two lattices are defined by the following two triplets of reciprocal vectors: {[222], [−242], [−202]} and {1/3[111], 1/3[−24 − 2], [−202]}. It is well established [39] that the CSL (DSC) of the reciprocal lattices is the reciprocal lattice of the DSC (CSL) of the two lattices, in the real space. The DSC lattice vectors, in the real space, are the geometrically possible Burgers vectors of dislocations in the interfaces. A mathematical derivation leads to the following DSC lattice vectors: 1/3[111], 1/6[−12 − 1] and 1/2[−101] or their combination. The most likely ones are dictated by energy considerations.

The composite electron diffraction pattern recorded along the zone axis $[-1-11]\delta // [-101]\gamma$ (Fig. 2) puts in prominent position the relationship between the twin-related variants, from the one hand, and the K-S orientation between the two γ_s variants and the δ matrix on the other hand.

3.5. X-ray spectroscopy microanalysis

In an attempt to assess the composition of γ_s phase, to establish the distribution of the alloying elements and to compare it to that of the ferritic matrix, microanalysis was performed using energy dispersive X-ray spectroscopy (EDS). Analyses were carried out in the thinnest areas of the sample, very close to the electrochemical hole. For the quantitative analysis, the *K* edge of the various elements (Fe, Cr, Ni, Mo, Mn and Si) was used. The quantification of the EDS spectra used for the Fe, Cr, Mo and Mn peak shapes was acquired from standards for a least-squares fitting and *k* factor calculation. For the statistical analysis, all the spectra for which the χ^2 of the fit was <4 were kept and even in this case the deviation of calculated concentration was always less than 3–5%. This uncertainty can be considered as a normal error inherent to the method used for quantification. Under these circumstances, the obtained results show that the chemical composition of the austenite is homogeneous from particle to particle. The different results of the chemical analysis are listed in Table II.

TABLE II Elemental partitioning of ferrite and austenite phases

	Elements (wt%)					
Phases	Fe	Mo	Cr	Mn	Ni	Si
$\delta(l)$	65.5	1.3	24.6	3.4	4.6	0.6
$\gamma_s(l)$	63.2	2.0	19.8	4.3	10.3	0.4
$\gamma_s(h)$	62.6	1.4	14.7	5.3	15.9	0.1
$\gamma_s(r)$	62.7	1.9	19.8	4.6	10.5	0.5
$\delta(r)$	65.6	1.6	24.5	3.6	4.2	0.5
γ_s(*untwinned*)	65.9	2.1	22.5	3.6	5.2	0.7

Concentrations of the alloying elements were recorded with the electron beam located, as indicated in Fig. 1, on the left (l), on the right (r) and on the habit (h) plane of γ_s particles. The results are compared with those of the surrounding (l, r) δ matrix and of the untwinned γ particles (Fig. 5).

Microanalysis of the γ_s phase was carried out with the twinning plane approximately parallel to the electron beam in order to maximize the volume of twin-related variants within the interaction volume. Since the electron beam had a spot size higher than 35 nm, the interaction volume defined by the beam clearly extended well into the twin-related variants. In fact, the focused electron beam has straddled the interface between the twin-related variants and the recorded results represent a weighted average of compositions.

Compared with the chemical composition obtained from the adjacent δ-ferrite, the twin-related variants and untwinned particles are enriched in Ni and depleted in Cr. The evolution of minor elements (Mo, Mn and Si) the levels of which are relatively small and outside experimental error, is also in the right way. However, it is interesting to note the opposite fluxes of BCC (Cr, Mo, Si) and FCC (Ni, Mn) stabilising elements in the γ_s particles. These fluxes are symmetrical when one moves from the median zone towards the borders of γ_s particle. This median zone which is parallel to (111) twin plane is more deficient in Cr and enriched in FCC stabilising elements (Ni, Mn) than the other regions of the γ_s particle. One may point out in passing that the median zone could also be a precipitation site for the τ-phase studied in detail elsewhere [17]. In this connection, bright field TEM image (Fig. 5) shows a particle of τ-phase taking place at the twin plane of the γ_s particle. The clear-cut difference in chemical composition between the austenite (twin-related and untwinned austenite particles) and the ferritic matrix implies without any doubt that the austenite formation does not occur by a diffusionless process.

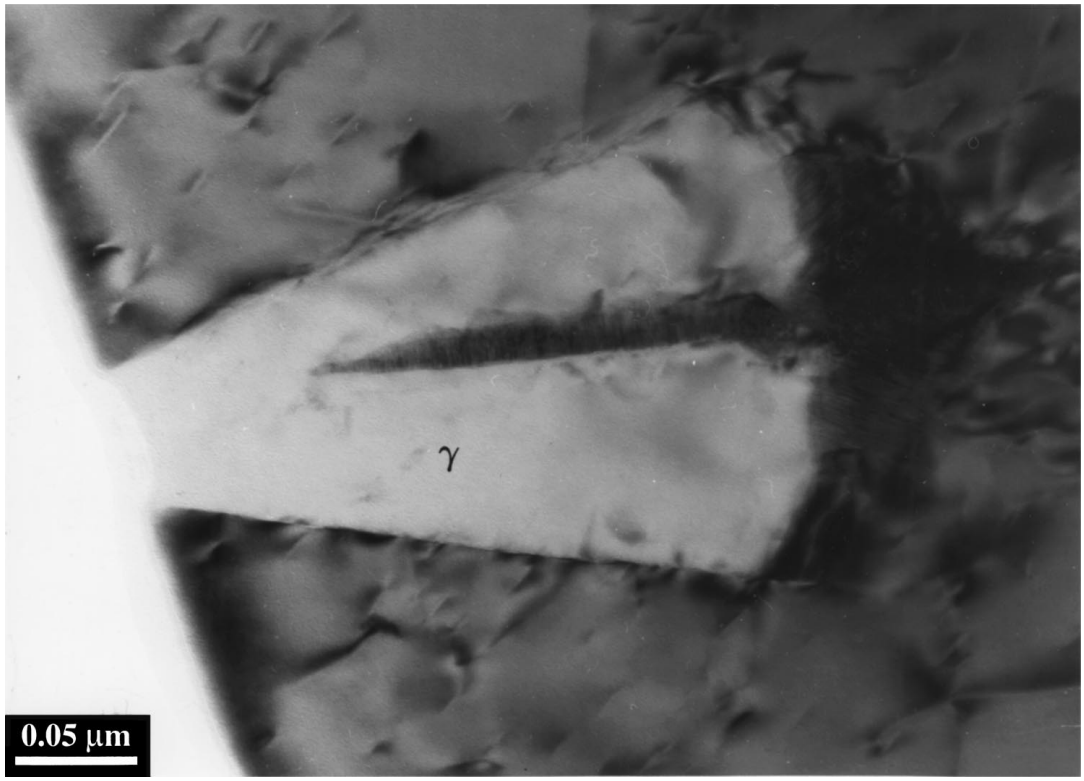

Figure 5 Bright field TEM micrograph showing a particle of τ-phase taking place at the twin plane of the γ_s particle.

4. Discussion

Chemical analysis points out that the twin-related γ_s particles are richer in FCC stabilising Ni and Mn elements with a shape less developed than that of the untwinned ones (Fig. 4). This attribute is related to the fact that the chemical composition of the untwinned particle is closer to that of the δ matrix making its development easier than the twin-related variants. It is also of interest to notice that the untwinned particles are less present than the twinned ones. This is basically due to the fact that the twin-related austenite has a lower activation energy barrier for nucleation. All this goes to indicate that the untwinned particle precipitation occurs by a nucleation and growth process while the twin-related particles take place in the matrix by a different and more complex mechanism.

In the light of TEM and EDS experimental results, it may be inferred that the γ_s formation operates through the following steps: i) enrichment of {110}-planes in ferrite with γ-forming elements by diffusion, ii) double shear to change from BCC (δ) to FCC (γ) lattice, iii) twinning of the FCC (γ) structure to reduce local strains and formation of γ bi-crystals, iv) growth of the twinned γ_s towards the ferritic matrix by volume diffusion. These different steps will be discussed briefly in turn:

- Enrichment of (110)-planes in ferrite with γ-forming elements by diffusion: The median zone which is parallel to (111) twin plane is more deficient in Cr and enriched in FCC stabilising element (Ni, Mn) than the other regions of the γ_s particle. This feature strongly supports the assumption that the median zone of the particle has been formed beforehand. This brings us to assume that in the early stage of γ_s precipitation, the (110)-ferritic planes are enriched with γ-forming elements by diffusion. This segregation of FCC stabilising element in (110)-planes is to be considered as a nucleation site, which will transform in (111)γ by double shear mechanism.
- Double shear to change BCC(δ) to FCC(γ): It is suggested that the precipitation of γ_s austenite is produced via a double shear nucleation mechanism in the early stage of the transformation. The double shear allows the BCC (δ) $\rightarrow$ FCC (γ) lattice transformation and leads to the stacking of the compact austenitic (111) planes. This double shear is carried out with the help of dislocations, the nature of which could be related to Shockley dislocations on the close packed planes of BCC and FCC lattices of the ferrite and austenite, respectively. The double shear nucleation mechanism based on the application of matrix theory to point lattices has been developed and will be detailed in a forthcoming paper [40].
- Twinning of the FCC γ structure to reduce local strains and formation of γ bi-crystals: The double shear is subsequently followed by a twinning, which develops an interface, the twin boundary, i.e. the median (111) plane. However, the twin is produced by the passage of a Shockley partial dislocation over every one of the (111) close packed austenitic planes. The fact that every γ_s precipitate is twinned supports the idea that the twinning mechanism is an intrinsic part of the structure and plays an important role in the self accommodation of the transformation strains as rightly emphasized by Xiao and Dahmen for α-TiO_2 precipitates in sapphire matrix [35].

The interest of both the double shear and the twinning is to explain the reduction of the activation energy barrier, thereby favouring the nucleation of the austenitic bi-crystals to the detriment of the untwined particles.

- Growth of the twinned γ_s towards the ferritic matrix by volume diffusion: Analysis of the elemental partitioning (Table II) of ferrite and austenite indicates clearly that the growth of the developed twin-related variants, i.e. the γ_s particle, takes place in the ferritic matrix by volume diffusion process.

5. Conclusion

TEM observation and electron diffraction experiments indicate that the very fine γ_s particles, throughout the δ matrix grains, are austenite and different from the one found at high temperature. The γ_s particles adopting spearhead-like morphology are, in point of fact, formed with two plates in twin-related configuration. The twinning plane separating the two variants is, in fact, not a midrib of the martensitic austenite as referred to in a previous study, suggesting that the precipitation is controlled by a diffusionless transformation [19]. The fact that every γ_s precipitate is twinned suggests that the twinning mechanism is an intrinsic part of the structure and plays an important role in the self-accommodation of the transformation strains.

The crystallographic results, in conjunction with the group theory and the clear-cut difference in chemical composition between the matrix and the second γ_s-phase imply, with certainty, that γ_s precipitation does not occur by a diffusionless process. It is suggested that the formation of γ_s particles occurs via an enrichment of (110)-planes in ferrite with γ-forming elements in the early stage of the transformation followed by a double shear mechanism, which transforms (110)-ferritic planes to (111)-austenitic planes. The twinning of the FCC structure leads to the formation of γ_s bi-crystals the growth of which involves a volume diffusion of the alloying elements.

The γ_s–phase obeys Kurdjumov–Sachs orientation relationship (K-S) with the ferritic matrix. A deviation from the exact K-S relationship is brought to light. It is related to the studied duplex stainless steel purity. The morphology adopted by the γ_s–phase does not correspond to symmetry-dictated extremum. However the absence of the symmetry–dictated extremum should be related to the chemical composition equilibrium of the two phases: austenite and ferrite.

A continuing investigation is to be started by characterizing the orientation relationships against the chemical composition equilibrium, i.e. the kinetic of the austenite formation in a duplex stainless steel whose composition must be controlled.

Acknowledgements

One of the authors (A. R.) is grateful to Dr P. Ruterana (Ecole Polytechnique de Lausanne, Swizerland; Present adress: LERMAT, Caen, France) for the chemical analysis by EDS and for the HREM observations.

References

1. R. M. DAVISON and J. M. REDMOND, *Mater. Performance* **29** (1990) 57.
2. H. KIESHEYER, in Proceedings of the International Conference on Stainless Steels' 91 (The Iron and Steel Institute of Japan, Chiba, Japan, 1991) p. 1148.
3. V. J. DIGGS, W. D. BUSKO and C. M. SCHILLMOLLER, in "Proceedings of the International Conference on Duplex Stainless Steels'91," Vol. 2, edited by J. Charles and S. Bernhardsson (Les Editions de Physique, Les Ulis, 1991) p. 1163.
4. D. J. A. FRUYTIER, in "Proceedings of the International Conference on Duplex Stainless Steels'91," Vol. 1, edited by J. Charles and S. Bernhardsson (Les Editions de Physique, Les Ulis, 1991) p. 497.
5. I. TAMURA and Y. TOMOTA, in Proceedings of the Symposium on Mechanical Behaviour of Materials, (Japan Society of Materials Science, Kyoto, 1974) Vol. 2, p. 105.
6. J. FOCT, N. AKDUT and G. GOTTSTEIN, *Scripta Metall. Mater*. **27** (1992) 1033.
7. N. SRIDHAR, J. KOLTS and L. H. FLASCHE, *J. Metals* **37** (1985) 31.
8. T. MAGNIN and J. M. LARDON, *Mater. Sci. Eng. A* **104** (1988) 21.
9. S. BERNHARDSSON, J. OREDSSON and C. MARTENSON, in "Proceedings of the International Conference on Duplex Stainless Steels'82," edited by R. A. Lula (ASM, Metals Park, Ohio, 1983) p. 267.
10. J. C. PROUHEZE, J. C. VAILLANT, G. GUNTZ, B. LEFEBVRE, in "Proceedings of the International Conference on Duplex Stainless Steels'82," edited by R. A. Lula (ASM, Metals Park, Ohio, 1983) p. 247.
11. H. D. SOLOMON, in "Proceedings of the International Conference on Duplex Stainless Steels'82," edited by R. A. Lula (ASM, Metals Park, Ohio, 1983) p. 41.
12. J. CHARLES, in "Proceedings of the International Conference on Duplex Stainless Steels'91," Vol. 1, edited by J. Charles and S. Bernhardsson (Les Editions de Physique, Les Ulis, 1991) p. 3.
13. A. REDJAÏMIA, Thèse de Doctorat d'Etat, Institut National Polytechnique de Lorraine, Nancy, France, 1991.
14. A. REDJAÏMIA, G. METAUER, M. GANTOIS, *Scripta Metall. Mater*. **25** (1991) 1879.
15. R. LAGNEBORG, *Trans. Am. Soc. Metals* **60** (1967) 67.
16. A. MATEO, L. LLANES, M. ANGLADA, A. REDJAÏMIA, G. METAUER, *J. Mater. Sci*. **32** (1997) 4533.
17. A. REDJAÏMIA, P. RUTERANA, G. METAUER and M. GANTOIS, *Phil. Mag. A* **67**(5) (1993) 1277.
18. E. L. BROWN and G. GRAUSS, *Metall. Trans*. **14** (1983) 791.
19. J. CHANCE, W. COOP and K. J. GRADWELL, in "Proceedings of the International Conference on Duplex Stainless Steels'82," edited by R. A. Lula (ASM, Metals Park, Ohio, 1983) p. 377.
20. P. D. SOUTHWICK and R. W. K. HONEYCOMBE, *Metal Science* (1980) 253.
21. W. BOLLMANN, *Phys. Stat. Sol. (a)* **21** (1974) 543.
22. R. W. BALLUFI, A. BROKMANN and H. KING, *Acta Metall*. **30** (1982) 1453.
23. U. DAHMEN, *Acta Metall*. **30** (1982) 63.
24. R. PORTIER, D. GRATIAS, *J. Phys. Sup*. **43**(12) (1982) C4.
25. J. W. CAHN and G. KALONJI, in "Proceedings of the Conference on Solid-Solid Phase Transformations," edited by H. I. Aaronson, R. F. Sekereka, D. E. Laughlin and C. M. Waymann (Metall. Soc. AIME, Warrendale, 1982) p. 3.
26. M. J. BUERGER, "Elementary Crystallography" (Massachussetts Institute of Technology Press, Cambridge, 1978).
27. B. C. MUDDLE and I. J. POLEMAR, *Acta Metall*. **36** (1989) 777.
28. A. BENLAMINE, R. PORTIER, J. P. SENATEUR and F. REYNAUD, *Scripta Metall*. **19** (1985) 63.
29. F. C. PHILLIPS, "An Introduction to Crystallography," 4th ed. (Longman, Singapore, 1971).

30. P. D. SOUTHWICK, PhD thesis, Cambridge, 1982.
31. M. EL HAJJAJI, Thèse de Doctorat d'Etat, Université Claude Bernard-Lyon I, 1986.
32. J. M. PENISSON and G. REGHEERE, *Mater. Sci. Eng.* (1989) 199.
33. J. H. VANDER MERWE, in Proceedings of the Royal Society (Londres, 1949) Vol. 198, p. 205.
34. C. P. LUO, U. DAHMEN, M. J. WITCOMB, and K. H. WESTMACOTT, *Scripta Metall. Mater.* **26** (1992) 649.
35. S. Q. XIAO, U. DAHMEN, A. H. HEUER, *Phil. Mag. A* **75**(1) (1997) 221.
36. O. JOHARI and G. THOMAS, *Trans. AIME* **230** (1964) 597.
37. G. THOMAS and M. J. GORINGE, "Transmission Electron Microscopy of Materials," (John Wiley and Sons, New York, 1979).
38. W. BOLLMANN, "Crystal Defects and Crystalline Interfaces" (Springer, Berlin, 1974).
39. H. GRIMMER, *Scripta Metall* **8** (1974) 1221.
40. A. REDJAÏMIA and G. METAUER, to be published.

Received 8 February
and accepted 26 September 2000